crystals

MDPI

Article

Recent Insights into Protein Crystal Nucleation

Christo N. Nanev

Rostislaw Kaischew Institute of Physical Chemistry, Bulgarian Academy of Sciences, 1113 Sofia, Bulgaria; nanev@ipc.bas.bg; Tel.: +359-2-856-64-58; Fax: +359-2-971-26-88

Received: 27 April 2018; Accepted: 12 May 2018; Published: 17 May 2018

Abstract: Homogeneous nucleation of protein crystals in solution is tackled from both thermodynamic and energetic perspectives. The entropic contribution to the destructive action of water molecules which tend to tear up the crystals and to their bond energy is considered. It is argued that, in contrast to the crystals' bond energy, the magnitude of destructive energy depends on the imposed supersaturation. The rationale behind the consideration presented is that the critical nucleus size is determined by the balance between destructive and bond energies. By summing up all intra-crystal bonds, the breaking of which is needed to disintegrate a crystal into its constituting molecules, and using a crystallographic computer program, the bond energy of the closest-packed crystals is calculated (hexagonal closest-packed crystals are given as an example). This approach is compared to the classical mean work of separation (MWS) method of Stranski and Kaischew. While the latter is applied merely for the so-called Kossel-crystal and vapor grown crystals, the approach presented can be used to establish the supersaturation dependence of the protein crystal nucleus size of arbitrary lattice structures.

Keywords: protein crystal nucleation; thermodynamic and energetic approach; protein 'affinity' to water; solubility; balance between crystal bond energy and destructive surface energies; supersaturation dependence of the crystal nucleus size

1. Introduction

Crystallization is the most efficient and economical way of obtaining chemically pure compounds. That is why it is widely used in the pharmaceutical, fertilizer and sugar industries. Single crystal X-ray diffraction, being the most universal, powerful and accurate tool for biological macromolecule structure analysis and protein–substrate interactions, requires relatively large and well-diffracting crystals. However, the major stumbling stone in X-ray diffraction analysis of protein crystals is the lack of a recipe (or definite indications) for growing crystals of newly expressed proteins. The issue is finding conditions that make the homogeneously scattered protein molecules in a solution form stable crystal nuclei; once nucleated, the crystals continue growing spontaneously. Evidently, nucleation is the crucial step that determines the difference between success and failure in protein crystallization trials. Regardless of the numerous auxiliary crystallization tools employed, such as automation and miniaturization of crystallization trials by means of robots, Dynamic Light Scattering, crystallization screening kits, etc., it is researchers' creativeness and acumen that remain indispensable. Even with state-of-the-art tools, it is exceptionally challenging to probe the nucleation processes in real time. Only most recently, this problem has been addressed successfully by Van Driessche et al. [1]. Nevertheless, some of the most intimate moments of molecule-by-molecule assembly to form crystal nuclei are still elusive and require further elucidation.

Following the fundamental notion of a kink position (*Halbkristalllage* in German) introduced by Kossel [2] and Stranski [3], the Bulgarian scientists Stranski and Kaischew [4–6] were the first to apply a molecular kinetic (and energetic) approach to crystal nucleation. They proposed the

so-called mean work of separation (MWS) method. To calculate the MWS value, all of the different kinds of bonds (between the first, second and third neighboring crystal-building blocks) are counted separately, and each number is multiplied by the corresponding bonding energy. Then, the products are summed up, and the result is divided by the total number of blocks in the corresponding crystal element (crystal face, cluster edge). It has been argued that for vapor phase crystallization MWS value is equal to the chemical potential, taken with a negative sign, plus a substance and temperature dependent constant [7]. To calculate the work required (energy barrier) for nucleus formation, crystal bond energies are used as well. They are calculated by summing up the number of all intra-crystal bonds, the breaking of which is needed to totally disintegrate a crystal into all its constituting molecules. The same approach is used in the present study. Applying the MWS method to the so-called Kossel-crystal (a crystal build by small cubes held together by equal forces in a cubic primitive crystal lattice) allows the equilibrium crystal shapes to be determined.

A big advantage of the MWS method is its simplicity. It uses the relative bond energies between separate crystal building units instead of the absolute bond energy values, which frequently are unknown. However, the MWS method has two major drawbacks: it is applicable only to the Kossel-crystal model (existing extremely rarely in nature) and considers solely enthalpic effects. Perhaps it is for these very reasons that the MWS method is used rarely nowadays, even though it enables semi-quantitative studies of crystal nucleation and growth.

To find the critical nucleus size, Garcia-Ruiz established the balance between the cohesive energy (ΔG_v), which maintains the integrity of a crystalline cluster, and the sum of destructive energies (ΔG_s), which tend to tear up the crystal, i.e., $-\Delta G_v + \Delta G_s = 0$ [8]. Using a cubic primitive crystal lattice formed by spheres, the author equilibrated the number of bonds shared by the crystal building units with the number of dangling bonds at the crystal surface, pointing toward the solution. This corresponds to the classical nucleation theory where ΔG_v is proportional to the crystal volume while ΔG_s is proportional to its surface, and the critical nucleus size is determined from the compensation of the large surface energy, which is inherent for the undercritical molecule clusters, by the faster volume energy increase resulting from the rising crystal size. Garcia-Ruiz's intuitive approach accounts for the water molecules acting on the apexes and edges that exist on the polyhedral crystal nuclei but are absent on the droplets. His model shows that at the crystal vertices, water molecules pull protein molecules towards the solution from three (perpendicular) directions, at the crystal edges from two directions, and at the crystal face from one direction only.

Recently, Garcia-Ruiz's brilliant idea was been further elaborated [9]. When the system is undersaturated, i.e., crystallization is impossible, the protein 'affinity' to water molecules prevails over the crystallization propensity. Therefore, to evoke crystallization, it is necessary to impose supersaturation and the higher the latter, the more thermodynamically stable the crystal is, with respect to the solution. Thus, it is feasible to assume that the imposed supersaturation decreases the protein-to-water affinity, i.e., supersaturation diminishes the destructive energy (ψ_d) per bond. This means that the tendency to tear up the crystal depends on the degree of supersaturation in contrast to the cohesive energy per bond in the crystal lattice (ψ_b) which is supersaturation independent. This means that any supersaturation increase will lead to an increase in ψ_b/ψ_d ratio. On this basis, the critical nucleus size dependence on supersaturation has been determined (from the balance between the sum of all intra-crystal bonds and the sum of surface destructive energies) for the Kossel-crystal model [9].

The objective of the present work is to shed additional light on the thermodynamic and molecular aspects of the homogeneous nucleation of non-Kossel crystals, such as nucleation of protein crystals in solution. To determine the supersaturation dependent critical nucleus size, the crystal bond energy and the sum of supersaturation dependent surface destructive energies are equilibrated (referred to as EBDE) and compared to the MWS method. In view of the nature of lattice binding forces among huge biomolecules, only the first nearest neighbor interactions are considered. For simplicity purposes, equal bond energy interactions throughout the whole crystal are assumed. The consequences of the

highly anisotropic and multivalent interactions of proteins during crystal nucleation were considered elsewhere [10]. However, specifics of protein and small molecule crystal nucleation are kept in mind [11].

2. Equilibration of Crystal Bond Energy with Surface Destructive Energies (EBDE)

2.1. Thermodynamic Basis of EBDE and Definition of Protein-to-Water Affinity

In [9], ψ_d was loosely defined as accounting for entropy, including the sum of all nucleation disfavoring entropic contributions. All entropy increasing components (favoring crystal nucleation) were included in ψ_b. A more rigorous definition of protein-to-water 'affinity' which uses both nucleation process enthalpy and entropy is provided below.

Thermodynamics stipulates that enthalpy and entropy govern phase transition. In contrast to crystal nucleation from vapors, protein crystal nucleation evokes a simultaneous entropy change in both solutions and crystals [12]. Rearrangement and/or release of some associated water or trapping of even more water molecules occurs when protein molecules get together to form a new solid phase. Therefore, entropy accounts for the change in the number of molecules in both protein crystals and solutes. Many water molecules are released in the solution for each protein molecule bound into the crystal lattice. In the disordered bulk solvent, these water molecules have six degrees of freedom and increase the entropy of the whole crystallizing system, thus leading to a decrease in the Gibbs free energy of phase transition. Sometimes, the entropy gain resulting from the said water transfer is the main component in the driving energy for protein crystal nucleation. However, it is not only the release of water molecules from the contacting patches (during crystalline bonds formation) that affects crystallization thermodynamics. Being immobilized in the crystal lattice, protein molecules lose entropy due to the highly constrained translational and rotational degrees of freedom. In turn, protein molecule ordering (crystal nuclei formation) is stimulated by an entropy gain due to the newly acquired vibrational degrees of freedom that arise upon molecule attachment to the crystal. Together with the high crystallization enthalpy, entropy changes ensure the negative values of Gibbs free energy required for spontaneous crystallization are attained (for more details see [12,13]). The conformational entropy of residues involved in crystal contact has been recently reconsidered [14]. Simultaneously, study of hydrogen bonds, van der Waals contacts and electrostatic interactions has shown that hydrogen-mediated van der Waals interactions are the dominant force that maintains protein crystal lattice integrity. Unfortunately, however, non-Kossel crystal lattice analysis remains a theoretical challenge [13].

The relation between ψ_d and supersaturation ($\Delta\mu$) is derived via the protein-to-water 'affinity' (α) noting that the lesser the value of α, the lesser the crystal solubility (c_e). As a first approximation, proportionality with a constant κ is assumed:

$$\alpha = \kappa c_e. \tag{1}$$

Also noted is the equal probability of crystal nuclei formation and dissolution. This means that the nucleation process can be regarded as a reversible chemical reaction characterized by the equilibrium constant for crystallization (K_{eq}). Combining the standard Gibbs free energy (ΔG^o) for crystals,

$$\Delta G^o = \Delta H^o - T\Delta S^o, \tag{2}$$

where ΔH^o is the standard enthalpy change, and ΔS^o is the change in entropy of the nucleation process. T is the absolute temperature. The Gibbs free energy isotherm equation is

$$\Delta G^o = -RT\ln K_{eq},$$

and by denoting the universal gas constant as R, the following is obtained:

$$\ln K_{eq} = -(\Delta H^o/RT) + (\Delta S^o/R). \quad (3)$$

Considering the approximation suggested by Sleutel et al. [15] and assuming an ideal solution (i.e., the activity coefficient is a unit), the crystallization equilibrium constant (K_{eq}) can be represented as $K_{eq} \approx (c_e/c^o)^{-1}$, which gives

$$\ln(c_e/c^o) = (\Delta H^o/RT) - (\Delta S^o/R). \quad (4)$$

where $c^o = 1$ mol L^{-1} is the solution's concentration in the standard state. Thus, solubility, c_e, is expressed in terms of the change in the entropy and enthalpy of the nucleation process:

$$c_e = c^o \exp[(\Delta H^o/RT) - (\Delta S^o/R)], \text{ and} \quad (5)$$

$$\alpha = \kappa c^o \exp[(\Delta H^o/RT) - (\Delta S^o/R)]. \quad (6)$$

The protein crystal solubility, c_e (and hence, protein-to-water affinity, α), depends on the solution's composition, mainly the precipitant type and concentration, pH, and temperature. (Isothermal protein crystal nucleation is considered here.) The lesser the solubility (affinity), the larger the supersaturation at the same solution concentration, c:

$$\Delta\mu = k_B T \ln(c/c_e) = k_B T \ln\{c \exp[(\Delta S^o/R) - (\Delta H^o/RT)]/c^o)\} = k_B T \ln(\kappa c/\alpha), \quad (7)$$

where k_B is the Boltzmann constant.

It has been known for a long time that the disordered solvent phase fills the void between molecules in the protein crystal lattice [16]. The role of water included in protein crystals acting like an 'additional glue' to hold protein molecules together has been considered elsewhere [17] and is not within the scope of this paper.

2.2. Energetics of Protein Crystal Nucleation

From energetic point of view, it is evident why 3D nuclei are preferred over 2D nuclei built by the same number of molecules. A (forth) molecule arriving from solution bulk prefers to start forming a second layer (B) rather than attaching itself to the periphery of an already existing layer (A) (Figure 1). The reason is that by sitting in the hole between the three molecules of layer A, this molecule bonds to the others using energy $3\psi_b$. If it is to remain in layer A, it will acquire two bonds only, so it jumps and forms layer B (Figure 2). For the same reason, it is highly probable that a fifth molecule will attach itself to the opposite side of the molecule triplet (Figure 1). That is how the cluster of bond energy $9\psi_b$, arises, instead of the planar configuration of energy $7\psi_b$.

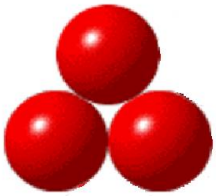

Figure 1. Three close-packed molecules form layer A.

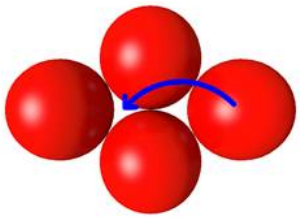

Figure 2. A molecule jumps to start formation of a second layer (B).

Typical 3D protein crystals are polyhedral, which is why crystal nuclei are assumed to have polyhedral shapes. The thermodynamic definition of protein-to-water affinity presented above assumes that crystals are stable entities, even though molecules at crystal vertexes and edges are connected more loosely than those at the crystal face. In view of the rather high supersaturations needed for protein crystal nucleation, this assumption is quite reasonable (and can be regarded as a justification for EBDE application).

Keeping in mind Garcia-Ruiz's postulate about water molecules pulling protein molecules at crystal vertexes towards the solution more strongly (from three different directions) than those at crystal faces, we notice that small molecule clusters, comprised of up to six molecules, have all of their molecules sitting at crystal vertexes. From the EBDE perspective, such small molecule clusters can be critical nuclei only provided supersaturation is very high. Table 1 shows the ψ_b/ψ_d ratio for the number (n) of molecules in a cluster; note that the supersaturation is decreasing from left to right. A 3D cluster formed by four molecules does not predetermine the lattice type—hexagonal closest packed (HCP) or face centered cubic (FCC)—of the growing crystal, while a 3D cluster, comprised of five molecules (three in layer A and one on each side, i.e., in two layers B), results in an HCP crystal lattice. A FCC structure requires larger clusters of at least six molecules. However, it is not only the energetic aspect that determines the crystal lattice type. Wukovitz and Yeates [18] have pointed out that an appropriate symmetry is mandatory for the crystallization of biological macromolecules.

Table 1. The ψ_b/ψ_d ratio for the number (n) of molecules in a cluster.

n	2	3	4(in 3D)	5(HCP)	6(FCC)
ψ_b/ψ_d	6	3	2	≈1.7	≈1.6

Using the MWS method, Kaischew [19] showed that homogeneously formed crystal nuclei are larger than heterogeneous nuclei. The reason for this is that the volume of a heterogeneous nucleus decreases to a degree that depends on the substrate's nucleation activity (see Figure 3). Energetically preferred 3D HCP (Figure 4) and 3D FCC crystals arise by adding three molecules in the (corresponding) holes at the top, and another three molecules at the bottom of an initial layer A of spheres arranged in the shape of a hexagon; all of the tetrahedral holes are covered in the HCP structure, and all of the octahedral holes are covered in the FCC crystals. The result is a three-fold rise in bond energy, up to $36\psi_b$, compared with $12\psi_b$ in the planar configuration, and the ψ_b/ψ_d ratio is calculated by EBDE (see Table 2, in which the supersaturation is decreasing from left to right).

The EBDE method benefits from crystallographic computer programs rendering the sums of bond energies ($\Delta G_v{}^3$) of arbitrary sized 3D crystals and the number (N_s) of surface atoms exposed to water destructive action. The advantage of crystallographic computer programs is that they are applicable to diverse crystal structures. Given as an example here are HCP crystals with <0100> edge lengths determined by the numbers (L) of the molecules in them. The ATOMS (Version 5.0.4, 1999) computer program is used to calculate $\Delta G_v{}^3$ and N_s for the crystals of a truncated bipyramidal shape. These crystals are geometrical homologues to the crystal (shown in Figure 5), with $L = 3$ (the three blue balls), in which the number of molecules (N_t) in the topmost and correspondingly, in the bottommost,

{0001} faces depend on L (so that for the differently sized crystals, $N_t = 3$ for $L = 2$ (Figure 4); $N_t = 7$ for $L = 3$ (Figure 5); $N_t = 12$ for $L = 4$; $N_t = 19$ for $L = 5$; $N_t = 27$ for $L = 6$, etc.).

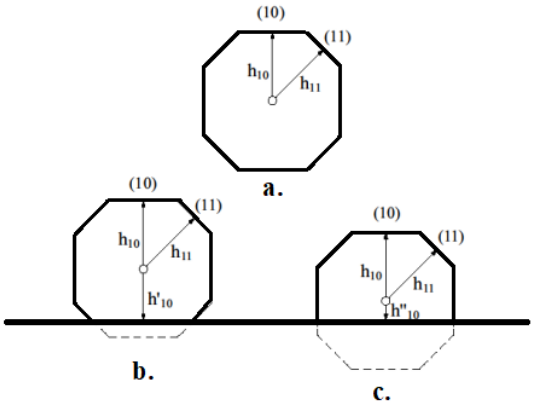

Figure 3. (**a**–**c**) 2D crystal nuclei: (**a**) homogeneous nucleus; (**b**,**c**) heterogeneously formed nuclei. Wulff's points are shown by small circles, and h_i denotes the corresponding distances (proportional to the respective surface free energies) used for the Currie–Wullf's constructions; the solid line represents the substratum surface.

Figure 4. Formation of a hexagonal closest packed (HCP) crystal.

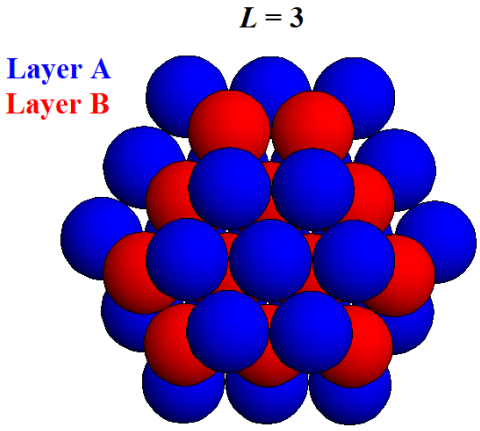

Figure 5. Top view of a five-layered HCP (truncated dihexagonal dipyramid) crystal, for which the two bottom layers are not seen. The crystal is formed on a closest packed monomolecular layer A of spheres (the blue balls) arranged into the shape of a complete hexagon with $L = 3$.

The plot of $\Delta G_v{}^3/\Delta G_s$ vs. L is shown in Figure 6. The reason for this plotting is that the energy balance ($-\Delta G_v + \Delta G_s = 0$) means $\Delta G_v/\Delta G_s = 1$, so the reciprocal of the ordinate value in Figure 6 (giving the corresponding ψ_b/ψ_d values) shows the decrease in supersaturation with an increase in L (Table 2). Here Garcia-Ruiz's postulate (that the molecules at the crystal vertexes are pulled towards the solution from three different directions, the molecules in the crystal edges are pulled from two directions, and the molecules in the crystal faces are pulled from one direction only) is also taken into account since it should apply to any crystal structure—water molecules are 'negligent' of the crystal lattice type. It is worth noting that the larger nucleus stands in equilibrium under the actual supersaturation until the larger ψ_b/ψ_d value in Table 2 (corresponding to higher supersaturation needed for formation the smaller crystal nucleus) is reached.

Table 2. The ψ_b/ψ_d ratio for the number (L) of molecules in the crystal edge.

L	2	3	4	5	6	7	8	9	10
ψ_b/ψ_d	1	0.43	0.25	0.17	0.13	0.10	0.087	0.07	0.06

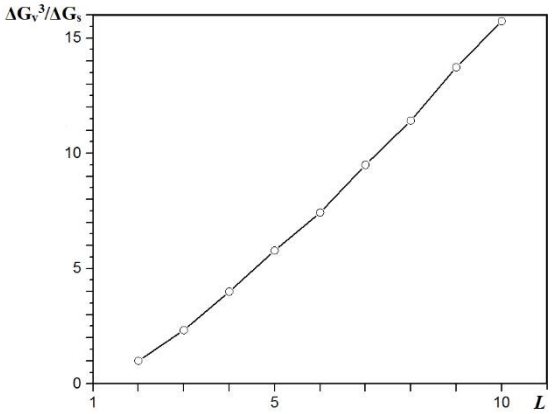

Figure 6. Plot of $\Delta G_v{}^3/N_s$ vs. L.

However, only crystals of modest size are of interest because though feasible from an energetic point of view, larger crystal nuclei are less likely to appear. There are kinetic reasons for this—bringing together a vast number of molecules via molecule-by-molecule assembly into a crystal nucleus involves very large fluctuations which in turn requires very long waiting times. For the same reason, the simplest crystal shapes are considered—any additional nuclei faces require a substantial increase in crystal size.

The discrete character of cluster-size alteration has been considered by Stoyanov, Milchev and Kaischew [20–23]. They established a step-wise, instead of a continuous, relationship between nucleus size and supersaturation, and a supersaturation interval instead of a fixed level of supersaturation corresponding to each critical nucleus.

3. MWS Method Application to Closest-Packed 3D Crystals; Comparison of EBDE and MWS

Crystallographic computer programs provide crystal lattice images and numerical data, in contrast to the classical MWS method which uses analytical expressions. Simple models of modestly sized 3D crystals with complete shapes were used to calculate the MWSs of faces forming the habitus of non-Kossel crystal nuclei, the reason being that incomplete crystalline clusters would have sites for subsequent attachment and formation of minimum surface free energy clusters. Considered herein are the closest-packed (HCP and FCC) crystals. To prepare such models, closest-packed monomolecular layers were stacked consecutively onto both sides of a basic A-layer. Three-layered (Figure 7), five-layered (Figure 5), etc. homologous HCP crystal nuclei with L = 3, 4, etc. were created. (It is worth noting that heaping 7 and more close-packed layers need larger foundations, i.e. larger

L values. As already mentioned however, a nucleus size limit is inevitable.) In contrast, to calculate the MWS of a {0001} crystal face, a whole upper mono-layer was stripped-off from the rest of the crystal. Then the layer disintegrated completely into its constituent molecules. The results made it obvious that MWS value calculations introduced uncertainty, caused by the alternatively stacked hexagonal and ditrigonal layers in the HCP crystals. This is why two different MWS values (but not one like by the Kossel-crystal) were calculated for the closest-packed surface layers. Oddly enough, depending on the type of surface layer to be disintegrated, the crystal stood in equilibrium with two different supersaturations.

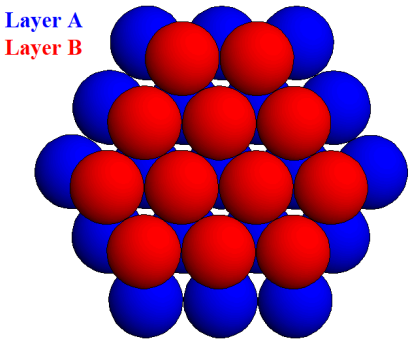

Figure 7. Top view of a three-layered HCP truncated dihexagonal dipyramid crystal (the bottom layer is unseen). The crystal is built by stacking the closest packed layers of spheres (the red balls) onto the single A layer (the blue balls, arranged into the shape of a complete hexagon with $L = 3$).

Well-known crystallography equations were applied for the MWS value calculations. Since each molecule in the closest-packed surface layer (regardless whether hexagonal or ditrigonal) is related to three molecules beneath it, the work (energy) needed for striping-off one such layer is always three times the number (z) of molecules in the layer. By denoting the number of molecules in the edge of a hexagonal layer by λ, we obtain

$$z = 3\lambda(\lambda - 1) + 1, \tag{8}$$

which gives z = 7, 19, 37, 61, 91, 127 ... for λ = 2, 3, 4, 5, 6, 7 ... respectively.

In addition, for the number (Z') of molecules in the ditrigonal layer, which is situated onto a hexagonal layer:

$$Z' = 3(\lambda - 1)^2, \tag{9}$$

which gives Z' = 3, 12, 27, 48, ... for λ = 2, 3, 4, 5 ... respectively.

A complete disintegration of the hexagonal and ditrigonal layers into their constituent molecules requires different amounts of work ($\Delta G_v{}^2$) which, in turn, implies two different MWS values. Though disintegration can be done in various ways, the result must be one and the same. Here, the crystallographic formula concerning the number of bonds in the hexagonal crystal layer is used:

$$\Delta G_v{}^2 = (3\lambda - 3)(3\lambda - 2). \tag{10}$$

Thus, the MWS value (W) for HCP crystals with hexagonal {0001} surface layers is

$$W = 3\psi_b + (3\lambda - 3)(3\lambda - 2)\psi_b/[3\lambda(\lambda - 1) + 1] = 3\psi_b + [9\lambda^2 - 15\lambda + 6]\psi_b/[3\lambda^2 - 3\lambda + 1]. \tag{11}$$

Neglecting (for $L \to \infty$) all numbers smaller than the quadratic terms in Equation (11) gives $W \to 6\psi_b$, i.e., the bonding energy of the molecule in a kink position.

The formula for ΔG_v^2 of ditrigonal layers is

$$\Delta G_v^2 = (3\lambda - 5)(3\lambda - 3), \quad (12)$$

and the MWS value (W) for HCP crystals with ditrigonal {0001} surface lattice planes is

$$W = 3\psi_b + (3\lambda - 5)(3\lambda - 3)\psi_b/3(\lambda - 1)^2 = 3\psi_b + [9\lambda^2 - 24\lambda + 15]\psi_b/[3\lambda^2 - 6\lambda - 3]. \quad (13)$$

Here, again, all numbers smaller than the quadratic terms in Equation (13) can be neglected for $L \to \infty$, and again, $W \to 6\psi_b$.

Relevant to the application of the MWS method to FCC crystals is the cubo-octahedron crystal shown in Figure 8 (which is composed by five layers, BCABC, and has eight equal octahedral faces of triangular shape, all of them containing six molecules). The EBDE method shows that this crystal can be a critical nucleus under supersaturation, which is determined from the ratio $\psi_b/\psi_d \approx 0.42$. It is almost equal to the ψ_b/ψ_d ratio for the HCP crystal shown in Figure 5 ($\psi_b/\psi_d \approx 0.43$, see Table 2). Note that the FCC crystal is comprised of 55 molecules, while the HCP crystal has two additional molecules.

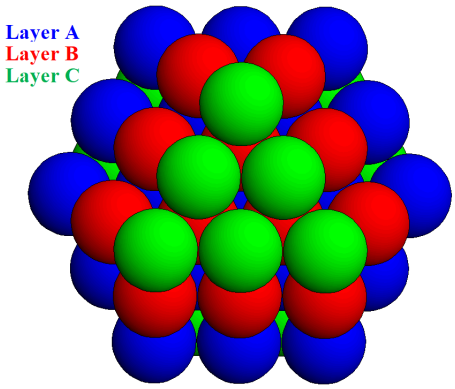

Figure 8. Top view of a five-layered face centered cubic (FCC) lattice crystal. It is formed on the closest packed single layer of A spheres (the blue balls) arranged in the shape of a complete hexagon with $L = 3$.

By applying the MWS method, we see that the stripping-off of the whole upper triangular layer {111} (containing green balls, Figure 8) requires work (energy) amounting to $18\psi_b$, while each layer here has a bond energy of $9\psi_b$. This gives a MWS value of $4.5\psi_b$. The cubic faces {100} are built from nine molecules of bond energy $12\psi_b$, and the bond energy of the front cubic face in Figure 8 to the layer beneath it is $32\psi_b$. This gives a MSW value $\approx 4.9\psi_b$. The different MWSs of the {111} and {100} faces indicate that, according to the MSW method, this crystal does not have an equilibrium shape.

The difficulties encountered with the highly symmetrical HPC and FCC crystals indicate that the MWS method has low applicability to less-symmetrical crystals. This notwithstanding, historically, the classical MWS method has played an important role in the crystal growth theory, regardless of being demonstrated merely on the Kossel-crystal model [24]. Markedly, present-day computer programs are capable of elucidating at least one of the basic notions used in the classical MWS method, namely the meaning of an 'infinitely' large crystal. The latter is used as a benchmark in Stranski-Kaischew's molecular kinetic theory. Figure 9 shows how the 'infinitely' large crystal size is approached asymptotically. Here, the N_b/N_a ratio (where N_b is the total number of bonds in the crystal and N_a is the number of molecules in the truncated HCP bipyramid) is plotted versus the crystal edge length, L. It is well-known that the N_b/N_a for a 12-coordinated molecule is six, and the bond energy of a molecule in the kink position is $6\psi_b$.

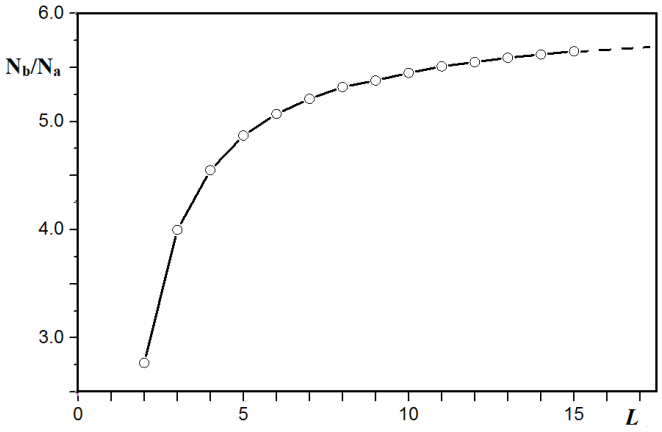

Figure 9. Plot of N_b/N_a ratio (where N_b is the total number of bonds in the crystal and N_a is the number of molecules in the truncated HCP bipyramid), which shows the influence of crystal vertexes and edges fading away with crystal enlargement. With $L \rightarrow \infty$ (L is the crystal edge length), the N_b/N_a ratio gradually approaches 6. Geometrical homologues to the HCP crystals like those in Figure 5 and in Figure 7 are considered.

4. Difference between Equilibrium and Growth Crystal Shapes

The nucleation stage predetermines the polymorphic crystal form (i.e., crystal lattice type) but not the habitus of a growing crystal (i.e., the type of faces on it). Crystal habitus depends on the growth rates of faces in normal directions. Historically, Stranski and Kaischew [25] were the first to recognize that the adsorption energy of a molecule at the middle of a crystal face can be used to characterize its growth rate. Later, Hartman and Bennema [26] proved that although dependent on the growth mechanism (via two-dimensional nucleation or spiral growth) and system conditions, face growth rate always increases with the increase in attachment energy per molecule on this crystal face. For instance, {110} faces grow faster than {100} and {111} faces because the steady-state growth shapes are determined by the number of their dangling bonds. The latter are five for {110} faces, four for {100} faces and three for {111} faces. In fact, ferritin crystals with the largest {111} faces have been observed most frequently—an indication that this is the slowest growing type of face in the normal direction and hence, the most morphologically important crystal face [27]. Using Atomic Force Microscopy, Yau and Vekilov [28] observed that near-critical-size apoferritin crystallites grow by attachment of molecules to the side {110} faces, thus forming a large {111} face. Growth of an apoferritin microcrystal consisting of three {111} layers of about 60 molecules in each was also detected. These nearly-critical crystallites were of quasi-planar (raft-like) shapes which is rather unusual for the FCC crystals.

5. Conclusions

An advantage of the EBDE method is that coupled with adequate computer programs, it can predict the nucleation of crystals of diverse lattice structures. As exemplified here with HCP crystals, modern computer programs (such as ATOMS) enable calculations considered unimaginable at the time of Stranski and Kaischew, over 80 years ago. Just as an example, the ordinate for $L = 10$ in Figure 9 is calculated for a HPC bipyramid crystal having $N_a = 2859$ atoms and $N_b = 15588$ bonds.

Founding: This work was co-financed by the National Science Fund of the Bulgarian Ministry of Science and Education, contract DCOST 01/22.

Acknowledgments: The author would like to acknowledge networking support by the COST Action CM1402 Crystallize. Also, the help of Kostadin Petrov is acknowledged. Crystallographic considerations and calculations, as well as Figures 5–9, were provided by him.

Conflicts of Interest: The author declares no conflict of interest. The founding sponsor had no role in the design of the study; in the collection, analyses, or interpretation of data; in the writing of the manuscript, and in the decision to publish the results.

References

1. Van Driessche, A.E.S.; Van Gerven, N.; Bomans, P.H.H.; Joosten, R.R.M.; Friedrich, H.; Gil-Carton, D.; Sommerdijk, N.A.J.M.; Sleutel, M. Molecular nucleation mechanisms and control strategies for crystal polymorph selection. *Nature* **2018**, *556*, 89–94. [CrossRef] [PubMed]
2. Kossel, W. Zur Theorie des Kristallwachstums. In *Nachrichten von der Gesellschaft der Wissenschaften zu Göttingen, Mathematisch-Physikalische Klasse*; Weidmannsche Buchhandlung: Berlin, Germany, 1927; pp. 135–143.
3. Stranski, I.N. Zur Theorie des Kristallwachstums. *Z. Phys. Chim. A* **1928**, *136*, 259–278. [CrossRef]
4. Stranski, I.N.; Kaischew, R.A. Über den Mechanismus des Gleichgewichtes kleiner Kriställchen, Part I. *Z. Phys. Chem. B* **1934**, *26*, 100–113.
5. Stranski, I.N.; Kaischew, R.A. Über den Mechanismus des Gleichgewichtes kleiner Kriställchen, Part II. *Z. Phys. Chem. B* **1934**, *26*, 114–116.
6. Stranski, I.N.; Kaischew, R.A. Über den Mechanismus des Gleichgewichtes kleiner Kriställchen, Part III. *Z. Phys. Chem. B* **1934**, *26*, 312–316.
7. Kaischew, R.A. Zur Theorie des Kristallwachstums. *Z. Phys.* **1936**, *102*, 684–690. [CrossRef]
8. Garcia-Ruiz, J.M. Nucleation of protein crystals. *J. Struct. Biol.* **2003**, *142*, 22–31. [CrossRef]
9. Nanev, C.N. On some aspects of crystallization process energetics, logistic new phase nucleation kinetics, crystal size distribution and Ostwald ripening. *J. Appl. Cryst.* **2017**, *50*, 1021–1027. [CrossRef]
10. Nanev, C.N. Kinetics and Intimate Mechanism of Protein Crystal Nucleation. *Prog. Cryst. Growth Character. Mater.* **2013**, *59*, 133–169. [CrossRef]
11. Nanev, C.N. Phenomenological Consideration of Protein Crystal Nucleation; the Physics and Biochemistry behind the Phenomenon. *Crystals* **2017**, *7*, 193. [CrossRef]
12. Vekilov, P.G.; Feeling-Taylor, A.; Yau, S.-T.; Petsev, D. Solvent entropy contribution to the free energy of protein crystallization. *Acta Cryst. D* **2002**, *58*, 1611–1616. [CrossRef]
13. Vekilov, P.G.; Chernov, A.A. The Physics of Protein Crystallization. *Solid State Phys.* **2003**, *57*, 1–147.
14. Dimova, M.; Devedjiev, Y.D. Protein crystal lattices are dynamic assemblies: The role of conformational entropy in the protein condensed phase. *IUCrJ* **2018**, *5*, 130–140. [CrossRef]
15. Sleutel, M.; Maes, D.; Van Driessche, A.E.S. Kinetics and Thermodynamics of Multistep Nucleation and Self-Assembly in Nanoscale Materials. In *Advances in Chemical Physics*; Chapter 9 What can Mesoscopic Level IN SITU Observations Teach us About Kinetics and Thermodynamics of Protein Crystallization? Nicolis, G., Maes, D., Eds.; Wiley-Blackwell: Malden, MA, USA, 2012; Volume 151, pp. 223–276.
16. McPherson, A. *Preparation and Analysis of Protein Crystals*; John Wiley & Sons: New York, NY, USA, 1982.
17. Nanev, C.N. Brittleness of protein crystals. *Cryst. Res. Technol.* **2012**, *47*, 922–927. [CrossRef]
18. Wukovitz, S.W.; Yeates, T.O. Why protein crystals favor some space-groups over others. *Nat. Struct. Biol.* **1995**, *2*, 1062–1067. [CrossRef] [PubMed]
19. Kaischew, R.A. Equilibrium shape and work for formation of crystal nuclei on substrates. *Common Bulg. Acad. Sci. Phys. Ser.* **1950**, *1*, 100–136.
20. Stoyanov, S. On the atomistic theory of nucleation rate. *Thin Solid Films* **1973**, *18*, 91–98. [CrossRef]
21. Milchev, A. Electrochemical phase formation on a foreign substrate—Basic theoretical concepts and some experimental results. *Contemp. Phys.* **1991**, *32*, 321–332. [CrossRef]
22. Milchev, A.; Stoyanov, S.; Kaischev, R.A. Atomistic theory of electrolytic nucleation: I. *Thin Solid Films* **1974**, *22*, 255–265. [CrossRef]
23. Milchev, A.; Stoyanov, S.; Kaischev, R.A. Atomistic theory of electrolytic nucleation: II. *Thin Solid Films* **1974**, *22*, 267–274. [CrossRef]
24. Tassev, V.L.; Bliss, D.F. Stranski, Krastanov, and Kaischew, and their influence on the founding of crystal growth theory. *J. Cryst. Growth* **2008**, *310*, 4209–4216. [CrossRef]
25. Stranski, I.N.; Kaischew, R.A. Gleichgewichtsformen homöopolarer Kristalle. *Z. Kristallogr.* **1931**, *78*, 373–385. [CrossRef]
26. Hartman, P.; Bennema, P. The attachment energy as a habit controlling factor: I. Theoretical considerations. *J. Cryst. Growth* **1980**, *49*, 145–156. [CrossRef]

27. Nanev, C.N. Bond selection during protein crystallization: Crystal shapes. *Cryst. Res. Technol.* **2015**, *50*, 451–457. [CrossRef]
28. Yau, S.-T.; Vekilov, P.G. Quasi-planar nucleus structure in apoferritin crystallization. *Nature* **2000**, *406*, 494–497. [PubMed]

© 2018 by the author. Licensee MDPI, Basel, Switzerland. This article is an open access article distributed under the terms and conditions of the Creative Commons Attribution (CC BY) license (http://creativecommons.org/licenses/by/4.0/).